International Journal of Pharmaceutics 401 (2010) 113–122

Contents lists available at ScienceDirect

International Journal of Pharmaceutics

journal homepage: www.elsevier.com/locate/ijpharm

Pharmaceutical Nanotechnology

Polyethylene sebacate–doxorubicin nanoparticles for hepatic targeting

Swati A. Guhagarkar[a], Rajiv V. Gaikwad[b], Abdul Samad[b], Vinod C. Malshe[c], Padma V. Devarajan[a,*]

[a] Department of Pharmaceutical Sciences and Technology, Institute of Chemical Technology, Matunga, Mumbai, Maharashtra 400 019, India
[b] Veterinary Nuclear Medicine Center, Department of Medicine, Bombay Veterinary College, Parel, Mumbai, Maharashtra 400 012, India
[c] Advanced Agro Tech., Thane, Maharashtra 400602, India

ARTICLE INFO

Article history:
Received 1 July 2010
Received in revised form 9 September 2010
Accepted 14 September 2010
Available online 18 September 2010

Keywords:
Nanoprecipitation
Doxorubicin
Polyethylene sebacate
Pullulan
Hepatic targeting

ABSTRACT

The present study discusses polyethylene sebacate (PES)–doxorubicin (DOX) nanoparticles (PES–DOX NP) using pullulan as asialoglycoprotein receptor (ASGPR) ligand for hepatic targeting. Pullulan, a hydrophilic polymer served as ligand and as stealth agent. PES–DOX NP were prepared by modified nanoprecipitation using PES and Gantrez AN 119 (Gantrez), as complexing agent in the organic phase, while DOX was dissolved in the aqueous phase. Pullulan was adsorbed on the formed nanoparticles (PES–DOX–PUL). Intimate association of PES and Gantrez, and ionic complexation of DOX with Gantrez (confirmed by FTIR), coupled with rapidity of nanoprecipitation resulted in nanoparticles with high entrapment efficiency and high drug loading. Nanoparticles were successfully freeze dried. Drug release from PES NP followed zero order kinetics. PES–DOX NP and PES–DOX–PUL exhibited low hemolytic potential and good serum stability. Comparative biodistribution study in rats using ^{99m}Tc labeled formulations revealed higher blood concentration and lower liver concentration of PES–DOX–PUL, confirming the long circulating nature of PES–DOX–PUL, and thereby the possibility of improved targeting to hepatocytes. Nanoparticles revealed lower DOX concentration in the heart suggestive of low cardiotoxicity. Our study presents a radically different yet simple approach for the design of PES–DOX nanoparticles with high drug loading for improved therapy in hepatic cancer.

1. Introduction

Hepatic cancer (HC) is one of the most widespread malignancies accounting for 4–5% of all human cancers, with nearly 5 million deaths occurring every year (Llovet et al., 2003; Schwartz and Llovet, 2008). Doxorubicin hydrochloride (DOX) is a drug of choice in the treatment of HC. Insufficient concentration at the tumor site coupled with cardiotoxicity, nephrotoxicity, myelosuppression and multiple drug resistance due to P-glycoprotein efflux and topoisomerase II resistance are serious limitations of current DOX therapy (Patil et al., 2008b). Enabled by their size and targetability, nanocarriers have been extensively studied to overcome the challenges in effective delivery of DOX. However conventional nanocarriers are rapidly cleared from circulation following intravenous injection mainly by kupffer cells of the liver and other macrophages (Brigger et al., 2002). Thus for efficient treatment of HC, a drug delivery strategy to enhance preferential uptake by hepatocytes with minimum kupffer cell uptake is essential (Xu et al., 2009). Long circulating targeted DOX nanocarriers could therefore provide important advantage in the treatment of HC.

Asialoglycoprotein receptor (ASGPR), also known as hepatic lectin represents a promising target for hepatocyte-specific delivery. ASGPR is predominantly present in large numbers on the sinusoidal cell membrane of hepatocyte and internalizes sugars such as galactose or lactose and glycoproteins with terminal galactose or N-acetylgalactosamine by endocytosis (Wu et al., 2002). ASGPR is reported to be over expressed on the surface of hepatocytes in patients with HC (Trouet and Jolles, 1984). Hence ASGPR targeting could provide a viable strategy for delivery of DOX in HC.

Several ligands such as asialo-feutin (Arangoa et al., 2003), asialo-transferrin, asialo-ceruloplasmin, asialo-lactoferrin, asialo-orosomucoid (Pathak et al., 2008), galactose and galactosylated or lactosylated residues including galactosylated cholesterol (Kawakami et al., 1998, 2000), galactosylated lipid (Wang et al., 2006), glycolipids (Sliedregt et al., 1999) and galactosylated polymers (Zanta et al., 1997) have been explored for selective targeting to hepatocytes. One such water soluble polysaccharide polymer pullulan, comprising of three α-1, 4-linked glucose molecules that are repeatedly polymerized at α-1, 6-linkages on terminals glucose is reported to be internalized by hepatocytes via ASGPR mediated endocytosis (Kaneo et al., 2001). Enhanced targeting to hepatocytes

* Corresponding author. Tel.: +91 22 33612201; fax: +91 22 33611020.
E-mail address: pvdevarajan@gmail.com (P.V. Devarajan).

0378-5173/$ – see front matter © 2010 Elsevier B.V. All rights reserved.
doi:10.1016/j.ijpharm.2010.09.012

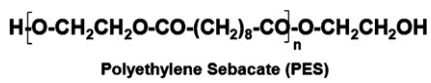

Fig. 1. Structure of polyethylene sebacate.

using pullulan–drug conjugates prepared by covalent bonding is reported (Hosseinkhani et al., 2002).

Polyethylene sebacte (PES), a new biodegradable polymer (Fig. 1) recently reported by our group has the advantages of ease of synthesis, good hydrolytic stability and low cost. Toxicity studies including genotoxicity and mutagenicity have confirmed safety of PES for biomedical and pharmaceutical applications (More et al., 2009). The objective of the present study is preparation and evaluation of DOX loaded PES nanoparticles (PES–DOX NP) for hepatic targeting using pullulan as ASGPR ligand. Pullulan, a hydrophilic polymer, when anchored on to nanoparticles could provide the dual advantage of stealth property and targeting to ASGPR by receptor mediated endocytosis. PES–DOX NP were prepared by modified nanoprecipitation using PES and Gantrez AN 119 (copolymer of methyl vinyl ether and maleic anhydride) as complexing agent in the organic phase, while DOX was dissolved in the aqueous phase.

2. Materials and methods

2.1. Materials

Doxorubicin hydrochloride was obtained from Hovid Sdn Bhd (Malaysia) as a gift sample. PES was synthesized in our laboratory (molecular weight: 9625). Gantrez AN 119 ISP (molecular weight 200,000) was obtained as a gift sample from Anshul Agencies (Mumbai, India). Tween 80, magnesium acetate, tetrahydrofuran (THF), and acetone were purchased from S.D. Fine Chemicals (Mumbai, India). Trehalose and pullulan (Hayashibara, Japan) were supplied as gift samples by Gangwal Chemicals Pvt Ltd (Mumbai, India). Distilled water was used throughout the experiments. All the other chemicals and reagents were either spectroscopic or analytical grade.

2.2. Nanoparticle preparation

PES–DOX NP were prepared by modified nanoprecipitation technique. PES (20 mg) and Gantrez AN 119 (Gantrez) were dissolved in 10 mL of THF and acetone (1:1). DOX (10 mg) and Tween 80 (10%, v/v) were dissolved in water. The organic phase was added drop-wise to the aqueous phase under magnetic stirring. Magnesium acetate tetrahydrate (1 mL of 0.5%, w/v solution) was added as a stabilizing agent for Gantrez after addition of the organic phase (Devarajan et al., 2005; Patil et al., 2008a). The resulting dispersion was stirred for a period of 4 h to ensure complete evaporation of the organic solvent. Nanoparticles were separated from the dispersion by centrifugation (Z36HK Hermle, Germany), at 20,000 rpm for 30 min. The resultant pellet was dispersed in distilled water/distilled water containing pullulan (nanoparticles:pullulan ratio 1:1) by probe sonication (DP120, Dakshin, Mumbai, India) for a period of 10 min with a 15 s on/off cycle.

2.3. Entrapment efficiency and drug loading

The supernatant obtained after centrifugation was suitably diluted and analyzed for free DOX by UV spectrophotometry (Shimadzu, Japan) at 478 nm. The % entrapment efficiency was calculated as follows:

$$\%\ \text{Entrapment efficiency} = \left\{[\text{DOX}]_{\text{total}} - [\text{DOX}]_{\text{supernatant}}/[\text{DOX}]_{\text{total}}\right\} \times 100$$

Drug loading was calculated using following formula (Subedi et al., 2009),

$$\%\ \text{Drug loading} = \frac{\text{amount of DOX entrapped in nanoparticles}}{(\text{amount of DOX added} + \text{amount of excipients added})} \times 100$$

2.4. Particle size

Particle size was determined by photon correlation spectroscopy on the N4 plus submicron particle size analyzer (Beckman Coulter, USA) at 25 °C. All measurements were taken by scattering light at 90°. The nanoparticulate dispersion was diluted with water (filtered through 0.22 μm membrane filter) to obtain final counts per second (intensity), 5×10^4–1×10^6 and the particle size recorded.

2.5. Zeta potential

The zeta potential of nanoparticles was determined using the Zeta sizer Nano ZS (Malvern Instruments Ltd, Malvern, UK). The pellet obtained after centrifugation of the nanoparticulate dispersion was washed repeatedly with distilled water to remove free drug and redispersed using sonication. The diluted sample was taken in capillary type cell and the zeta potential determined.

2.6. Transmission electron microscopy (TEM)

The morphology/shape of nanoparticles was determined following negative staining with uranyl acetate by TEM (CM 200 TEM/Philips/FEI, Inc., Briarcliff Manor, NY, USA). Imaging was performed on transmission electron microscope at a voltage of 200 kV having magnification of 0.23 nm. A drop of nanoparticle dispersion (1 mg/mL) was placed on Formvar®-coated copper grids (Ted Pella, Inc., Redding, CA) followed by the addition of a drop of 2% (w/v) uranyl acetate. After 3 min incubation at room temperature, excess liquid was drained, the grid air-dried and imaging conducted using the TEM.

2.7. In vitro drug release

The release of DOX from PES nanoparticles was determined by the dialysis bag method using the USP dissolution apparatus I, in phosphate buffer saline pH 7.4 (50 mL), at 50 rpm and 37 ± 0.5 °C. Nanoparticulate dispersion corresponding to 1 mg of DOX was filled in a dialysis bag (HIMEDIA®, molecular weight cut off 12,000–14,000 Da) and placed in the basket of the USP dissolution apparatus I. An aliquot of 5 mL was withdrawn at suitable time intervals and replaced with the same amount of medium. The samples were analyzed for DOX by UV spectrophotometry (Schimadzu, Japan) at 478 nm. DOX solution was used as control.

2.8. Freeze–thaw

Freeze–thaw study was carried out as a pre-test for screening type and concentration of cryoprotectant to be used during freeze drying. The concentration of nanoparticles was kept at 6 mg/mL. Nanoparticle dispersion (1 mL) was placed in the glass vials containing different type and concentrations of cryoprotectants and subjected to freezing at −40 °C for a period of 24 h in the deep freezer (Eclipse 400 RS Biotech, UK) followed by thawing at 28 °C. Particle size was determined by photon correlation spectroscopy

as mentioned in Section 2.4. Ratio of final particle size (S_f) to initial particle size (S_i) was calculated.

2.9. Freeze drying

Freeze drying of nanoparticles was carried out on a Labconco freeze dryer (FreeZone 4.5, USA). The nanoparticle dispersion (5 mL) was frozen at −40 °C for 12 h in a deep freezer (Eclipse 400 RS Biotech, UK) and then subjected to freeze drying. Sublimation lasted for 36 h at a vacuum pressure of 54×10^{-3} bar without heating, with the condenser surface temperature maintained at −54 °C. Freeze dried nanoparticles were reconstituted by suspending in 0.22 μm filtered water followed by bath sonication for a period of 10 min.

2.10. Fourier transform infrared (FT-IR) spectroscopy

Fourier transform infrared spectra of DOX, Gantrez, DOX–Gantrez physical mixture and DOX–Gantrez complex were recorded on a Perkin Elmer RX1 infrared spectrometer. Samples were crushed to a fine powder, mulled with anhydrous potassium bromide, compressed to form a thin transparent pellet and subjected to FTIR.

2.11. Differential scanning calorimetry (DSC)

Thermograms of DOX, Gantrez, DOX–Gantrez physical mixture and DOX–Gantrez complex were recorded by heating samples from 35 °C to 250 °C at a heating rate of 10 °C min^{-1} using an empty aluminum pan as the reference. Powdered samples were accurately weighed (5 mg) in aluminum pans, sealed and subjected to differential scanning calorimetry under nitrogen flow using a Perkin Elmer Pyris 6 DSC.

2.12. X ray diffraction (XRD)

X ray diffraction spectra of DOX, Gantrez, DOX–Gantrez physical mixture and DOX–Gantrez complex were recorded at room temperature using Philips Pro Expert diffractometer, with nickel filtered Cu Kα radiation operated at a voltage of 3 kV, 5 mA current, 4°/min scanning speed, and 5–40° (2θ) range.

2.13. In vitro hemolytic assay

A reported method was followed (Chen et al., 2008) to determine hemolytic potential of nanoparticles. Dispersion of PES–DOX NP and PES–DOX–PUL was diluted with phosphate buffer saline pH 7.4 to obtain concentrations equivalent to 0.05, 0.1, 0.2, 0.3, 0.4, and 0.5 mg/mL of DOX. Dispersion of blank PES NP was similarly diluted to serve as control. To 1.45 mL of each dilution, 50 μL of rat blood was added. Following incubation at 37 °C for 60 min, the samples were centrifuged at 5000 rpm for 10 min and the amount of released hemoglobin measured spectrophotometrically at a wavelength of 540 nm. Different concentrations of PES–DOX NP incubated by replacing blood with buffer served as control to nullify interference from DOX absorption at 540 nm. Phosphate buffer saline was used as the negative control and distilled water was used as the positive control. % Hemolysis was calculated using the formula:

$$\%\ \text{Hemolysis} = \frac{\text{Absorbance in the supernatant containing nanoparticles}}{\text{Absorbance in the supernatant containing distilled water}} \times 100$$

2.14. In vitro serum stability

The serum stability of PES–DOX NP and PES–DOX–PUL was evaluated by determining change in the particle size following incubation in serum over a period of 6 h. Freshly prepared PES–DOX NP and PES–DOX–PUL were mixed with rat serum (50%, v/v) in a ratio of 1:1 in an eppendorf tube and incubated at 37 ± 0.5 °C. At predetermined time intervals nanoparticles were evaluated for change in size. Particle size was determined by photon correlation spectroscopy as mentioned in Section 2.4.

2.15. Radiolabeling of DOX, PES–DOX NP and PES–DOX–PUL

DOX, PES–DOX NP and PES–DOX–PUL were labeled with ^{99m}Tc after reduction with stannous chloride. Briefly stannous chloride solution in 0.1 N HCl was added to ^{99m}Tc in normal saline (0.1 mg of stannous chloride per mci of ^{99m}Tc). This was followed by immediate addition of DOX/PES–DOX NP/PES–DOX–PUL and citrate buffer pH 7.2. The mixture was then agitated for 20 min on a shaker at 28 °C. Radiolabeling efficiency was determined by minor modification of a reported method (Reddy et al., 2004; Patil et al., 2008a). The radiolabeled formulation was spotted on a high performance thin layer chromatography (HPTLC) plate at a distance of 1 cm from the lower end and developed using acetone as the mobile phase. Solvent was allowed to travel 10 cm from the origin. The plate was removed, dried, and cut into two portions, lower one third and upper two third. The radioactivity in each part was determined using a gamma counter (I-125 Gamma Counter IC 4702). Radioactivity corresponding to the lower one third was regarded as (formulation) bound activity while the radioactivity corresponding to the upper two third was regarded as unbound (free) activity (R_f of ^{99m}Tc = 0.9). The percent radiolabeling efficiency was represented as percent ratio of bound activity to total activity. Stability of radiolabeled complex was determined by monitoring radiolabeling efficiency up to 6 h at 28 °C.

2.16. Biodistribution studies

Healthy female Sprague–Dawley rats with average body weight (BW) 200 ± 20 g were used for the study. The animals were maintained under standard laboratory conditions (14 h:10 h dark/light cycle, a temperature of 22 ± 2 °C and 50–70% humidity). Pelleted feed and water were provided ad libitum. The animal ethics committee, Bombay Veterinary College, Mumbai, India had approved the experimental protocol for study. Animals were anesthetized by injecting a cocktail of ketamine hydrochloride (50 mg kg^{-1}) and xylazine hydrochloride (10 mg kg^{-1}), intramuscularly, 20 min prior to study.

The animals were placed prone on a Millennium MPS Acquisition System, (Multipurpose Single Head Square Detector) Gamma Camera fitted with Low Energy General Purpose (LEGP) collimator. The distance of the collimator to table was maintained at 95 cm for all acquisitions. DOX (5 mg kg^{-1}) as radiolabeled DOX, PES–DOX NP and PES–DOX–PUL (approx. 500 μCi) was injected intravenously into the tail vein. For the purpose of determining total injected dose the radioactivity of the syringe before and after dosing was determined using a Dose Calibrator (Capnitech). The total injected dose was estimated by subtracting radioactivity after dosing from radioactivity before dosing. At each hour, up to 5 h post dosing, static images were recorded for a period of 1 min each at 1.33× zoom. All the static images were stored digitally in a 256 × 256 matrix.

At the end of 5 h animals were sacrificed, and heart, spleen, lungs, liver, stomach and intestine were isolated. The organs were washed with saline, blot dried and weighed. The radioactivity in each organ as well as in the whole body after removal of all the

Table 1
Entrapment efficiency, particle size, drug loading and zeta potential of PES–DOX NP (mean ± S.D., $n = 3$).

DOX (mg)	Gantrez (mg)	PES (mg)	Molar ratio of ionic charges (Gantrez AN/DOX)	Particle size (nm)	% Drug loading	% Entrapment efficiency	Zeta potential (mV)
10	0	20	0	145.9 ± 3.9	0.04 ± 0.02	0.14 ± 0.08	–
	1.25		1	334.5 ± 21.9	14.6 ± 0.98	45.68 ± 5.3	−18 ± 0.7
	2.5		2	292.3 ± 14.4	25.7 ± 0.52	83.65 ± 1.7	−22 ± 1.9
	5		4	102.8 ± 15.08	21.6 ± 0.62	75.92 ± 2.4	−22.1 ± 1.7
	10		8	107.2 ± 17.1	15.7 ± 0.48	63.00 ± 1.8	−25 ± 0.17

organs was determined using the Dose Calibrator (Capnitech) and corrected for physical decay. The % injected dose g^{-1} of organ was calculated.

2.17. Statistical analysis

All data in the tables and figures are expressed as mean ± standard deviation and mean ± standard error respectively. Statistical analysis was performed using the one-way ANOVA with Dunnet's test and Student's t tests. $p < 0.05$ was the criterion for statistical significance.

3. Results

3.1. Nanoparticle preparation and characterization

Organic solvents with high polarity like acetone are known to promote the formation of small size nanoparticles by facilitating rapid diffusion of the organic phase into the aqueous phase (Legrand et al., 2007). PES is insoluble in acetone, hence a mixture of acetone and THF was employed as organic phase. Negligible entrapment was seen in the absence of Gantrez. However inclusion of Gantrez in the organic phase resulted in drastic increase in entrapment efficiency (Table 1). The high entrapment efficiency is attributed to ionic complexation between Gantrez and DOX (Fig. 2). FT-IR spectroscopy confirmed ionic complexation between DOX and Gantrez. Absence of NH^{3+} stretching vibrations (3160–2300 cm^{-1}) of DOX in the transmission infrared spectrum of DOX–Gantrez complex indicated ionic complexation between the protonated amine group of DOX and the free carboxyl group of Gantrez (Fig. 3). DSC and X-RD spectra of DOX–Gantrez complex revealed absence of endotherm and reduced crystallinity of DOX respectively (Fig. 4).

Maximum entrapment was seen at Gantrez/DOX ratio of 2 (Fig. 5). Further, increase in Gantrez concentration, led to decrease in entrapment efficiency. Likewise particle size was also influenced by Gantrez concentration and was found to decrease with increase in the polymer concentration (Table 1). Nanosize (102 nm) and high drug loading (20%, w/w) was obtained at a Gantrez/DOX ratio 4. Negative zeta potential values can be attributed to presence of Gantrez. Further zeta potential values of PES–DOX-NP (−22.1 ± 2.4 mV) and PES–DOX–PUL (−21.9 ± 0.5 mV) were comparable. However during isolation of nanoparticles by centrifugation the particle size increased to ~200 nm (Vauthier et al., 2008). TEM image of PES–DOX NP revealed near spherical morphology and a size which correlated well with the photon correlation spectroscopy measurements (Fig. 6).

3.2. In vitro drug release

Rapid dialysis of DOX in solution was observed, with about 100% of drug being released at the end of 2 h (Fig. 7). Drug release from PES–DOX NP on the other hand was found to be slow with only 50% of the drug released in about 5 h. Drug release from nanoparticles was best explained by zero order release kinetics for 90% drug release ($r^2 = 0.998$ for PES–DOX NP and 0.997 for PES–DOX–PUL). According to the Korsmeyer–Peppas equation the value of diffusion release exponent n dictates drug release mechanism. Drug release in zero order, non-fickian diffusion and fickian diffusion is represented by $0.89 < n < 1$, $0.45 < n < 0.89$, and $n = 0.45$ respectively (Merchant et al., 2006). The value of n was found to be 0.94 and 0.96 for PES–DOX NP and PES–DOX–PUL respectively indicating near zero order release. Further the release profiles of PES–DOX NP and PES–DOX–PUL were comparable ($F2$ value = 66.01).

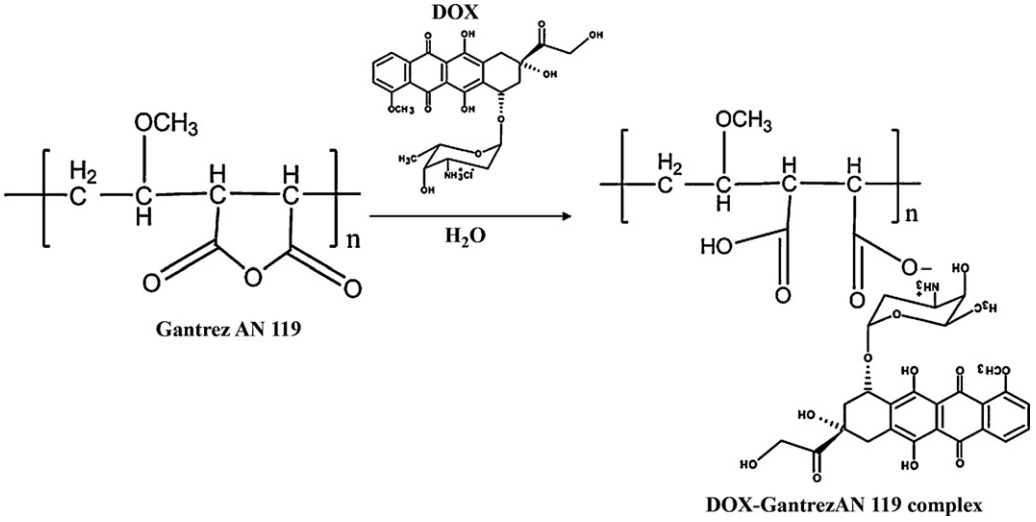

Fig. 2. Schematic representation of formation of DOX–Gantrez complex.

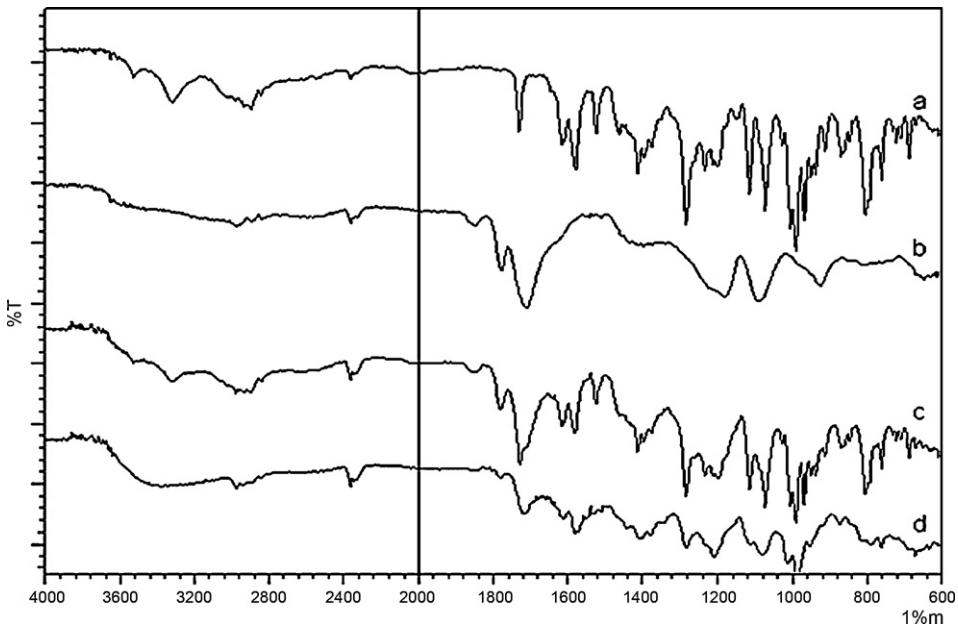

Fig. 3. FT-IR spectra of (a) DOX, (b) Gantrez AN 119, (c) DOX: Gantrez AN 119 physical mix and (d) DOX: Gantrez AN 119 complex.

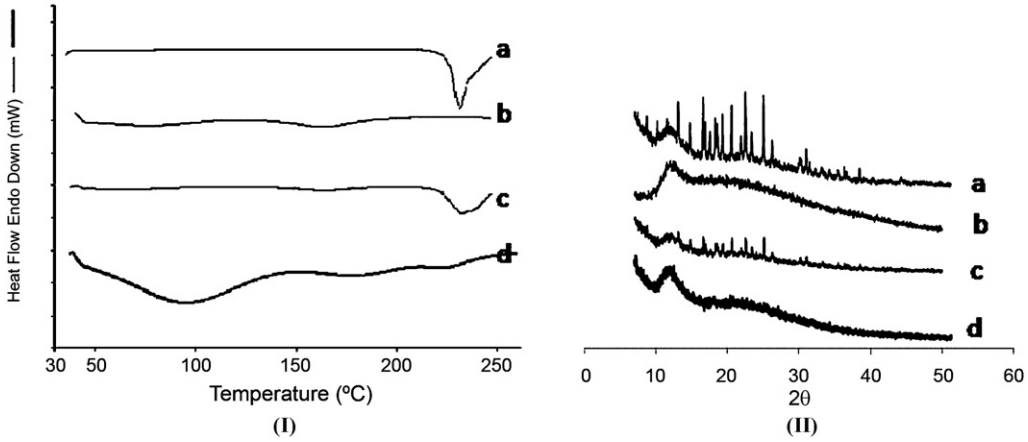

Fig. 4. DSC thermograms (I) and XRD spectra (II) of (a) DOX, (b) Gantrez AN 119, (c) DOX: Gantrez AN 119 physical mix and (d) DOX: Gantrez AN 119 complex.

3.3. Freeze–thaw and freeze drying

The influence of trehalose, sucrose, mannitol and dextrose concentrations of 2.5%, 5%, 10%, 15% (w/v) on S_f/S_i was evaluated (Table 2). Without cryoprotectant nanoparticles revealed irreversible aggregation upon freeze thawing. With fructose and dextrose as cryoprotectants, S_f/S_i ratio were $<1 \pm 0.3$ (Saez et al., 2000) at all concentrations studied while trehalose prevented

Table 2
Effect of cryoprotectant type and concentration on particle size of PES–DOX NP after freeze–thaw (mean ± S.D., $n = 3$).

Cryoprotectant	Concentrations (%, w/v)	Initial mean size (S_i) (nm)	Final mean size (S_f) (nm)	S_f/S_i
Trehalose	2.5	200.1 ± 9.1	297.1 ± 2.2	1.48
	5		300.1 ± 1.2	1.49
	10		256.7 ± 2.4	1.28
	15		234.6 ± 1.0	1.17
Fructose	2.5	211.2 ± 13.7	228.5 ± 0.05	1.08
	5		199.7 ± 1.4	0.94
	10		194.0 ± 5.1	0.91
	15		209.7 ± 19.4	0.99
Mannitol	2.5	186.8 ± 9.3	>1000	–
	5		580.3 ± 20.4	3.1
	10		326.1 ± 21.4	1.74
	15		236.5 ± 7.9	0.78
Dextrose	2.5	183.9 ± 7.1	179.4 ± 3.6	0.97
	5		184.5 ± 17	1.003
	10		184.9 ± 8.6	1.005
	15		186.0 ± 7.7	1.01

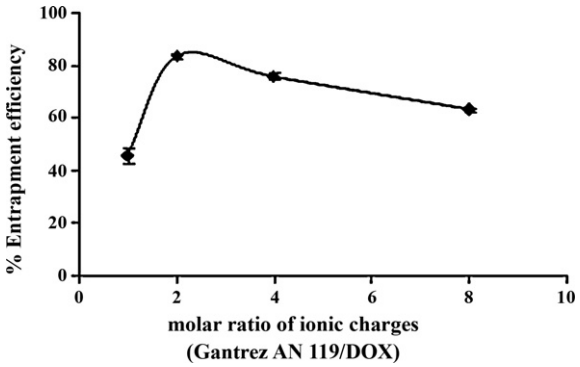

Fig. 5. Effect of molar ratio of ionic charges (Gantrez AN 119/DOX) on % entrapment efficiency of DOX.

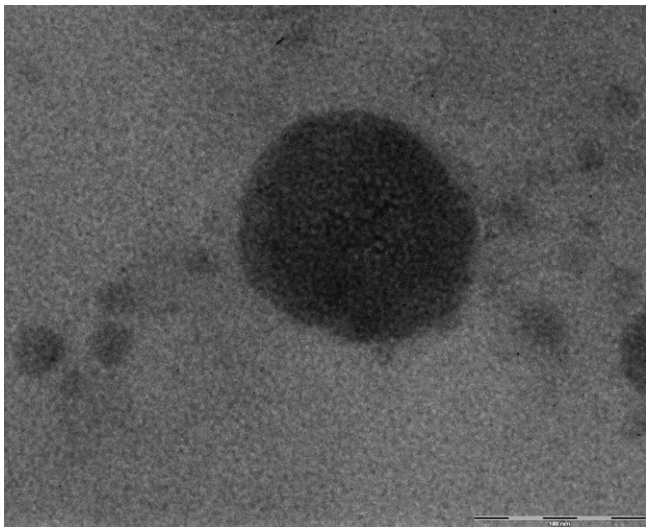

Fig. 6. TEM image of PES–DOX NP.

increase in size of nanoparticles at a concentration of >5% w/v. Mannitol revealed protection only at high concentration of 15% w/v. Based on the results of freeze–thaw studies trehalose, fructose, mannitol and dextrose at a concentration of 15% (w/v) were selected for freeze drying. While trehalose revealed formation of amorphous powder upon freeze drying, softening and collapse of the frozen matrix was seen with fructose, mannitol and dextrose.

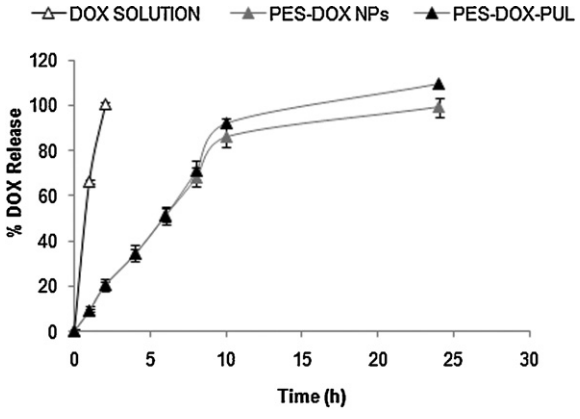

Fig. 7. In vitro release profile of DOX solution, PES–DOX NP and PES–DOX–PUL (mean ± S.E., $n = 3$).

Table 3
Particle size of PES–DOX NP on freeze drying (mean ± S.D., $n = 3$).

Cryoptotectant % w/v	Initial mean Size (S_i) nm	Final mean Size (S_f) nm	S_f/S_i
Trehalose	215.6 ± 1.8	>1000	–
Trehalose (15%) + lutrol F 68 (0.5%)	214.6 ± 8.6	344.6 ± 8.1	1.60
Trehalose (15%) + lutrol F 68 (1%)	204.9 ± 18.9	300 ± 10.5	1.46
Trehalose (15%) + lutrol F 68 (2%)	209.6 ± 5.9	284.3 ± 15.9	1.35

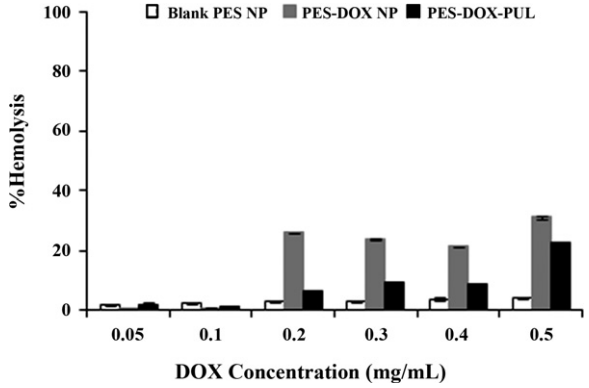

Fig. 8. In vitro hemolysis of blank PES NP, PES–DOX NP and PES–DOX–PUL (mean ± S.E., $n = 3$).

The particle size was however large (>1000 nm). Addition of lutrol F 68 to the nanoparticle dispersion prior to freeze drying enabled control of this growth in size (Table 3).

3.4. In vitro hemolytic assay

Blank PES nanoparticles revealed negligible hemolysis (<4%) whereas hemolytic potential of PES–DOX NP was found to be dependent on DOX concentration (Fig. 8). Further PES–DOX–PUL was found to be less hemolytic when compared to PES–DOX NP.

3.5. In vitro serum stability

Both PES–DOX NP and PES–DOX–PUL revealed good stability in serum for a period of 6 h (Fig. 9). Although increase in particle size was observed after 5 h, the average particle size did not exceed 240 nm and hence nanoparticles may be considered as adequately stable.

3.6. Radiolabeling of DOX, PES–DOX NP and PES–DOX–PUL

TLC revealed radiolabeling efficiency of >90% for DOX, PES–DOX NP and PES–DOX–PUL. Moreover ^{99m}Tc labeled complex was found to be stable for a period of 6 h (Fig. 10).

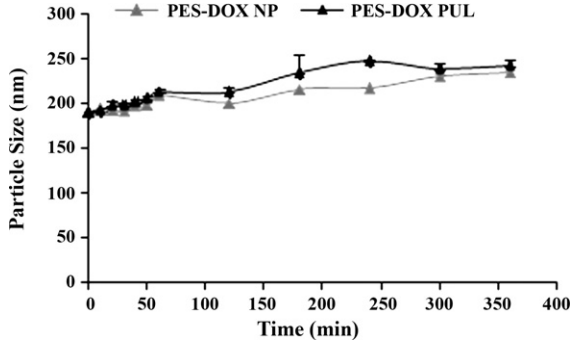

Fig. 9. In vitro serum stability of PES–DOX NP and PES–DOX–PUL (mean ± S.E., $n = 3$).

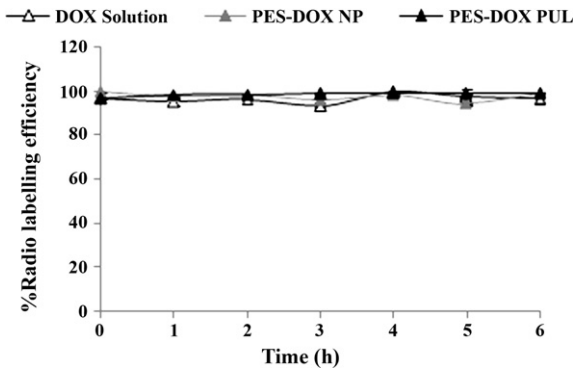

Fig. 10. Radiolabeling efficiency of DOX solution, PES–DOX NP and PES–DOX–PUL (mean ± S.E., $n = 3$).

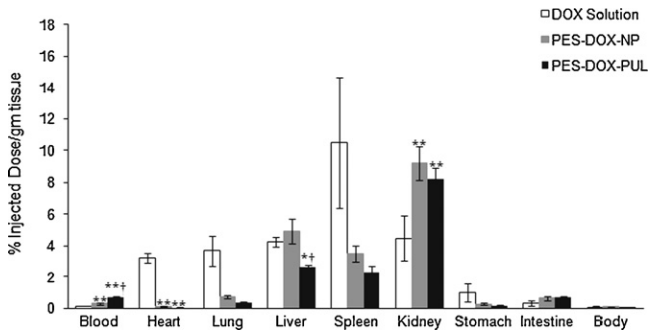

Fig. 12. Comparative biodistribution profile of DOX solution, PES–DOX NPs and PES–DOX PUL 5 h post administration (mean ± S.E., $n = 4$, $^{**}p < 0.01$ between DOX solution and other formulations, $^{*}p < 0.05$ between DOX solution and PES–DOX–PUL, $^{\dagger}p < 0.05$ between PES–DOX NP and PES–DOX–PUL).

3.7. Biodistribution studies

Gamma scintigraphic images and comparative biodistribution profiles of DOX solution, PES–DOX NP and PES–DOX–PUL 5 h post administration are depicted in Figs. 11 and 12 respectively. PES–DOX–PUL revealed significantly lower liver concentration and ($p < 0.05$) and high blood concentration ($p < 0.01$) compared to PES–DOX NP and DOX solution. Heart and lung concentrations with nanoparticles were significantly lower ($p < 0.01$) and kidney concentrations higher ($p < 0.01$) compared to DOX solution. The concentration in stomach and intestine were comparable whereas negligible concentrations were found in the body.

4. Discussion

Amongst the different methods reported for nanoparticle preparation, nanoprecipitation method developed by Fessi et al. remains widely studied (Fessi et al., 1989; Moinard-Checot et al., 2006; Legrand et al., 2007). Although nanoprecipitation is a simple, easy to perform one step procedure, it suffers from the disadvantage of low entrapment efficiency for water soluble drugs, due to leaching into the aqueous non solvent phase (Barichello et al., 1999; Govender et al., 1999; Bilati et al., 2005). Moreover the hydrophobic nature of PES increases the challenges in loading of hydrophilic DOX.

Reported attempts to enhance entrapment efficiency of DOX in particulate carriers have focused on decreasing its aqueous solubility. Complexation with anionic polymers such as dextran sulfate (Wong et al., 2004) and hydrolyzed polymer of epoxidized soybean oil (Wong et al., 2006) have been studied for improving entrapment of DOX in polymer–lipid hybrid nanoparticles. Chavanpatil et al. (2007) reported use of anionic surfactant dioctyl sodium sulfoscuccinate (Aerosol OT) to enhance entrapment of DOX in sodium alginate nanoparticles. Tewes et al. (2007) reported high entrapment efficiency of DOX in poly (lactide-co-glycolide) (PLGA) prepared by oil-in-water or water-in-oil-in-water emulsion method by modulating polarity of DOX. The present study discusses a radical approach in the preparation of nanoparticles by nanoprecipitation, wherein, water soluble ionic drug DOX is directly dissolved in the aqueous nonsolvent phase to achieve high entrapment and high loading in the hydrophobic PES nanoparticles using Gantrez as complexing agent.

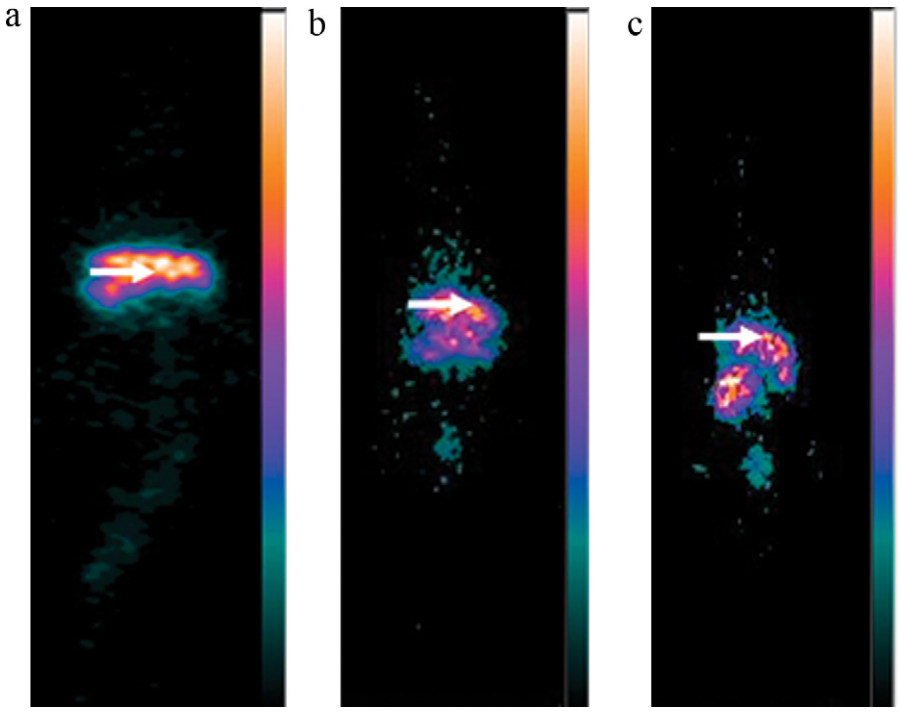

Fig. 11. Gamma scintigraphic images depicting biodistribution profile post 5 h administration of (a) DOX solution (b) PES–DOX NP (c) PES–DOX–PUL (→ = liver marker).

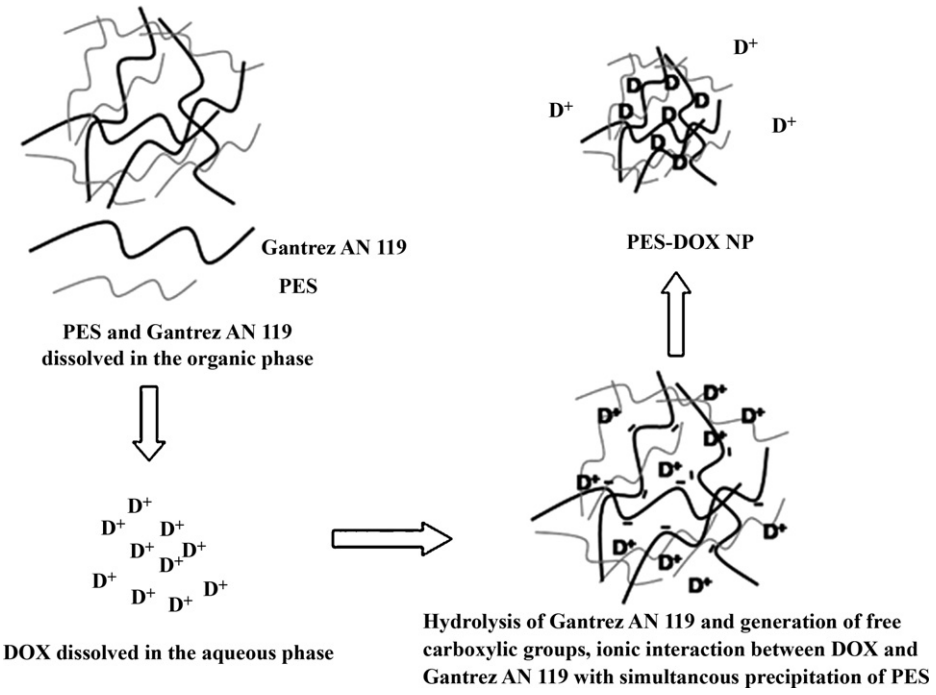

Fig. 13. Schematic representation of DOX loading into PES nanoparticles in presence of Gantrez AN 119.

DOX loading in nanoparticles is schematically depicted in Fig. 13. The polymers PES and Gantrez when dissolved in the organic phase are in a state of maximum extension and in intimate contact. Rapid nanoparticle formation is governed by Marangoni effect or diffusion stranding phenomenon which results from interfacial turbulence that exists at the solvent–non solvent interface leading to variations in the flow, diffusion and surface tension resulting in formation of small nanoparticles (Quintanar-Guerrero et al., 1998; Bilati et al., 2005). When the organic phase is added to the aqueous phase diffusion of organic solvent and counter diffusion of water induces desolvation and instantaneous precipitation of the polymers PES and Gantrez. Rapidity of nanoprecipitation and intimate contact of PES and Gantrez preclude leaching of Gantrez into the aqueous phase. Further on contact with the aqueous phase Gantrez undergoes instantaneous hydrolysis at the anhydride bond to generate free carboxylic groups which complexes with the quaternary ammonium group of DOX, to form a more lipophilic DOX–Gantrez complex. This complex preferentially partitions into the hydrophobic PES nanoparticles to enable high drug loading. Additionally steric constraints in the long chain polymer Gantrez provides more void spaces for incorporation of DOX (Layre et al., 2006). The high drug loading of hydrophilic drug DOX in PES nanoparticles is therefore, a cumulative effect of the above processes.

In the standard nanoprecipitation technique the drug is solubilized in the organic phase with the help of a polar solvent or water. This, on the one hand, significantly limits the amount of water soluble drug that can be incorporated in the organic phase, and moreover could result in larger nanoparticles. Repeat nanoprecipitation method suggested to enhance entrapment of water soluble proteins and peptide molecules in nanoparticles (Gao et al., 2007) is tedious and time consuming. Our modified nanoprecipitation method differs radically from reported methods, in that, despite DOX being dissolved in the aqueous phase we obtained high entrapment efficiency (>70%) and high drug loading (~20%).

Gantrez played an important role in influencing entrapment efficiency and particle size. The effect of Gantrez on entrapment efficiency is analogous to that observed by Wong et al. (2004) in preparation of polymer–lipid hybrid nanoparticles using dextran sulfate as an anionic polymer. Decrease in particle size observed with increasing Gantrez concentration can be attributed to the amphiphilic nature and surface active property of the polymer (Legrand et al., 2007).

The release pattern of cytotoxic drug is critical, as continuous exposure to low levels of cytotoxic drugs may induce P-gp overexpression, rendering the cancer cells more drug resistant. However rapid release of drug is also undesirable as it can lead to systemic toxicity (Wong et al., 2007). Sustained drug release of DOX from PES–DOX NP and PES–DOX–PUL can be considered as a desirable release profile.

Freeze–thaw studies were conducted as a pretest, to identify the optimum cryoprotectant for freeze drying studies, as an excipient which cannot protect the nanoparticles during first step of freeze drying i.e. freezing; it is not likely to be an effective cryoprotectant (Date et al., 2010). Though all the cryoprotectants evaluated for freeze–thaw study were found to inhibit increase in particle size, only trehalose yielded a satisfactory freeze dried product. Superiority of trehalose over other sugar molecules is attributed to the higher glass transition temperature (De Jaeghere et al., 2000), low hygroscopicity, and absence of internal hydrogen bonding, which allows formation of hydrogen bonds with nanoparticles during freeze drying (Abdelwahed et al., 2006), thereby preventing aggregation. However as trehalose alone did not restrain increase in particle size upon freeze drying lutrol F 68 was added to nanoparticle dispersion prior to freeze drying to enable S_f/S_i ratios of $<1 \pm 0.3$. We have reported similar observations during freeze drying of silymarin loaded PES nanoparticles (Guhagarkar et al., 2009).

Nanoparticles intended for intravenous administration must be evaluated for their interaction with blood constituents to confirm their safety. Determination of hemolytic potential is one of the most common tests used to evaluate suitability of nanoparticles for intravenous applications. Blank PES nanoparticles revealed low hemolytic potential suggesting suitability of nanoparticles for intravenous administration. The lower hemolytic potential of PES–DOX–PUL, when compared to PES–DOX NP opens up the possibility, to administer doxorubicin at higher concentrations. The hydrophilic agent pullulan, would have minimized the interac-

tion between the nanoparticles with blood components. Changes in nanoparticle size in the presence of serum can be related to the adsorption of the serum protein on the nanoparticles (Han et al., 2006). This is of significance as particle size greatly influences the fate of nanoparticles in vivo. PES–DOX NP and PES–DOX–PUL revealed good serum stability with no significant change in particle size over a period of 6 h.

Lower liver concentration of PES–DOX–PUL compared to PES–DOX NP and DOX solution, suggests bypass of the kupffer cells, while high blood concentration of PES–DOX–PUL, when compared to PES–DOX NP and DOX solution, confirms the long circulating property and stealth effect of pullulan. The long circulating property coupled with kupffer cell bypass presents the possibility of enhanced uptake by hepatocytes, by increasing number of passes through liver. DOX is known to cause toxicity to myocardial cell membrane by lipid peroxidation, which causes oxidative stress, resulting in necrosis of cells (Singal and Iliskovic, 1998). Entrapment of DOX in nanoparticles (PES–DOX NP and PES–DOX–PUL) revealed negligible heart concentration of DOX compared to DOX solution ($p < 0.01$) indicating the possibility of lower cardiotoxicity (Gabizon et al., 1982; Herman et al., 1983). Although higher concentration of DOX was seen in the kidneys, the advantages of targeting DOX and the reduced cardiac levels could outweigh the severity of kidney toxicity (Manil et al., 1994, 1995).

5. Conclusion

Our study presents a radical, yet simple, modified nanoprecipitation approach, for the preparation of PES–DOX nanoparticles with high entrapment efficiency and low particle size. Moreover, inclusion of pullulan as ASGPR ligand provides long circulating property, with the possibility of receptor mediated endocytosis, to target the ASGPR. Additional studies including pharmacokinetic and pharmacodynamic evaluation are planned to confirm enhanced targeting to hepatocytes.

Acknowledgments

We acknowledge Department of Biotechnology (DBT), Government of India for providing financial support for the project and research fellowship to Swati A. Guhagarkar. We wish to thank Indian Institute of Technology (IIT), Mumbai and Tata Institute of Fundamental Research (TIFR), Mumbai for TEM and X-RD studies respectively. Dr. Mahesh Pawar and Dr. Sonal from Bombay Veterinary College are acknowledged for the help in the biodistribution study.

References

Abdelwahed, W., Degobert, G., Stainmesse, S., Fessi, H., 2006. Freeze-drying of nanoparticles: formulation, process and storage considerations. Adv. Drug Deliv. Rev. 58, 1688–1713.

Arangoa, M.A., Duzgunes, N., Tros de Ilarduya, C., 2003. Increased receptor mediated gene delivery to the liver by protamine–enhancedasialofetuin–lipoplexes. Gene Ther. 10, 5–14.

Barichello, J.M., Morishita, M., Takayama, K., Nagai, T., 1999. Encapsulation of hydrophilic and lipophilic drugs in PLGA nanoparticles by the nanoprecipitation method. Drug Dev. Ind. Pharm. 25, 471–476.

Bilati, U., Allémann, E., Doelker, E., 2005. Development of a nanoprecipitation method intended for the entrapment of hydrophilic drugs into nanoparticles. Eur. J. Pharm. Sci. 24, 67–75.

Brigger, I., Dubernet, C., Couvreur, P., 2002. Nanoparticles in cancer therapy and diagnosis. Adv. Drug Deliv. Rev. 54, 631–651.

Chavanpatil, M.D., Khdair, A., Patil, Y., Handa, H., Mao, G., Panyam, J., 2007. Polymer–surfactant nanoparticles for sustained release of water soluble ionic drugs. J. Pharm. Sci. 96, 3379–3389.

Chen, W., Gua, B., Hao, W., Pan, J., Lua, W., Hou, H., 2008. Development and evaluation of novel itraconazole-loaded intravenous nanoparticles. Int. J. Pharm. 362, 133–140.

Date, P.V., Samad, A., Devarajan, P.V., 2010. Freeze–thaw: a simple approach for prediction of optimal cryoprotectant for freeze drying. AAPS Pharm. Sci. Technol. 11, 304–313.

De Jaeghere, F., Allémann, E., Feijen, J., Kissel, T., Doelker, E., Gunny, R., 2000. Freeze-drying and lyopreservation of diblock and triblock poly(lactic acid)–poly(ethylene oxide) (pla–peo) copolymer nanoparticles. Pharm. Dev. Technol. 5, 473–483.

Devarajan, P.V., Sonavane, G.S., Doble, M., 2005. Computer-aided molecular modeling: a predictive approach in the design of nanoparticulate drug delivery system. J. Biomed. Nanotechnol. 1, 375–383.

Fessi, H., Puisieux, F., Devissaguet, J.-P., Benita, A.N., 1989. Nanocapsule formation by interfacial polymer deposition following solvent displacement. Int. J. Pharm. 55, R1–R4.

Gabizon, A., Dagan, A., Goren, D., Barenholz, Y., Fuks, Z., 1982. Liposomes as in vivo carriers of adriamycin: reduced cardiac uptake and preserved antitumor activity in mice. Cancer Res. 42, 4734–4739.

Gao, H., Wang, Y.N., Fan, Y.G., Ma, J.B., 2007. Conjugates of poly(DL-lactide-co-glycolide) on amino cyclodextrins and their nanoparticles as protein delivery system. J. Biomed. Mater. Res. A 80, 111–122.

Govender, T., Stolnik, S., Garnett, M.C., Illum, L., Davis, S.S., 1999. PLGA nanoparticles prepared by nanoprecipitation: drug loading and release studies of a water soluble drug. J. Control. Release 57, 171–185.

Guhagarkar, S.A., Malshe, V.C., Devarajan, P.V., 2009. Nanoparticles of polyethylene sebacate: a new biodegradable polymer. AAPS Pharm. Sci. Technol. 10, 935–942.

Han, H.D., Shin, B.C., Choi, H.S., 2006. Doxorubicin-encapsulated thermosensitive liposomes modified with poly(N-isopropylacrylamide-co-acrylamide): drug release behavior and stability in the presence of serum. Eur. J. Pharm. Biopharm. 62, 110–116.

Herman, E.H., Rahman, A., Ferrans, V.J., Vick, J.A., Schein, P.S., 1983. Prevention of chronic doxorubicin cardiotoxicity in beagles by liposomal encapsulation. Cancer Res. 43, 5427–5432.

Hosseinkhani, H., Aoyama, T., Ogawa, O., Tabata, Y., 2002. Liver targeting of plasmid DNA by pullulan conjugation based on metal coordination. J. Control. Release 83, 287–302.

Kaneo, Y., Tanaka, T., Nakano, T., Yamaguchi, Y., 2001. Evidence of receptor-mediated hepatic uptake of pullulan in rats. J. Control. Release 70, 365–373.

Kawakami, S., Fumoto, S., Nishikawa, M., Yamashita, F., Hashida, M., 2000. In vivo gene delivery to the liver using galactosylated cationic liposomes. Pharm. Res. 17, 306–313.

Kawakami, S., Yamashita, F., Nishikawa, M., Takakura, Y., Hashida, M., 1998. Asialoglycoprotein receptor mediated gene transfer using novel galactosylated cationic liposomes. Biochem. Biophys. Res. Commun. 252, 78–83.

Layre, A.-M., Couvreur, P., Chacun, H., Aymes-Chodur, C., Ghermani, N.-E., Poupaert, J., Richard, J., Requier, D., Gref, R., 2006. Busulfan loading into poly(alkyl cyanoacrylate) nanoparticles: physico-chemistry and molecular modeling. J. Biomed. Mater. Res. B: Appl. Biomater. 79, 254–262.

Legrand, P., Lesieur, S., Bochot, A., Gref, R., Raatjes, W., Barratt, G., Vauthier, C., 2007. Influence of polymer behaviour in organic solution on the production of polylactide nanoparticles by nanoprecipitation. Int. J. Pharm. 344, 33–43.

Llovet, J.M., Burroughs, A., Bruix, J., 2003. Hepatocellular carcinoma. Lancet 362, 1907–1917.

Manil, L., Couvreur, P., Mahieu, P., 1995. Acute renal toxicity of doxorubicin (adriamycin)-loaded cyanoacrylate nanoparticles. Pharm. Res. 12, 85–87.

Manil, L., Davin, J.C., Dechenne, C., Kubiak, C., Foidart, P., Couvreur, P., Mahieu, P., 1994. Uptake of nanoparticles by rat glomerular mesangial cells in vitro and in vivo. Pharm. Res. 11, 1160–1165.

Merchant, H.A., Shoaib, H.M., Tazeen, J., Yousuf, R.I., 2006. Once-daily tablet formulation and in vitro release evaluation of cefpodoxime using hydroxypropyl methylcellulose: a technical note. AAPS Pharm. Sci. Technol. 7, E1–E6.

Moinard-Checot, D., Chevalier, Y., Briançon, S., Fessi, H., Guinebretière, S., 2006. Nanoparticles for drug delivery: review of the formulation and process difficulties illustrated by the emulsion–diffusion process. J. Nanosci. Nanotechnol. 6, 2664–2681.

More, A., Chilgunde, S., Patil, P., Kamble, J., Malshe, V., Vanage, G., Devarajan, P., 2009. Polyethylene sebacate: genotoxicity, mutagenicity evaluation and application in periodontal drug delivery system. J. Pharm. Sci. 98, 4781–4795.

Pathak, A., Vyas, S.P., Gupta, K.C., 2008. Nano-vectors for efficient liver specific gene transfer. Int. J. Nanomed. 3, 31–49.

Patil, R.R., Gaikwad, R.V., Samad, A., Devarajan, P.V., 2008a. Role of lipids in enhancing splenic uptake of polymer–lipid (lipomer) nanoparticles. J. Biomed. Nanotechnol. 4, 359–366.

Patil, R.R., Guhagarkar, S.A., Devarajan, P.V., 2008b. Engineered nanocarrier of doxorubic: a current update. Crit. Rev. Ther. Drug Carrier Syst. 25, 1–61.

Quintanar-Guerrero, D., Allémann, E., Fessi, H., Doelker, E., 1998. Preparation techniques and mechanisms of formation of biodegradable nanoparticles from preformed polymers. Drug Dev. Ind. Pharm. 24, 1113–1128.

Reddy, L., Reddy, H., Sharma, R.K., Chuttani, K., Mishra, A.K., Murthy, R.R., 2004. Etoposide-incorporated tripalmitin nanoparticles with different surface charge: formulation, characterization, radiolabeling, and biodistribution studies. AAPS J. 6 (Article 23).

Saez, A., GuzmaÂn, M., Molpeceres, J., Aberturas, M.R., 2000. Freeze-drying of polycaprolactone and poly(D,L-lactic-glycolic) nanoparticles induce minor particle size changes affecting the oral pharmacokinetics of loaded drugs. Eur. J. Pharm. Biopharm. 50, 379–387.

Schwartz, J.D., Llovet, J.M., 2008. Molecular targeting in hepatocellular carcinoma. In: Kaufman, H.L., Wadler, S., Antman, K. (Eds.), Cancer Drug Discovery and Development: Molecular Targeting in Oncology. Humana Press, Totowa, NJ, pp. 165–210.

Singal, P.K., Iliskovic, N., 1998. Doxorubicin-induced cardiomyopathy. N. Engl. J. Med. 339, 900–905.

Sliedregt, L.A.J.M., Rensen, P.C.N., Rump, E.T., Van Santbrink, P.J., Bijsterbosch, M.K., Valentijn, A.R.P.M., Van der Marel, G.A., Van Boom, J.H., Van Berkel, T.J.C., Biesen, E.A.L., 1999. Design and synthesis of novel amphiphilic dendritic galactoside for selective targeting of liposomes to the hepatic asialoglycoprotein receptor. J. Med. Chem. 42, 609–618.

Subedi, R.K., Kang, K.W., Choi, H.-K., 2009. Preparation and characterization of solid lipid nanoparticles loaded with doxorubicin. Eur. J. Pharm. Sci. 37, 508–513.

Tewes, F., Munnier, E., Antoon, B., Okassa, L.N., Cohen-Jonathan, S., Marchais, H., Douziech-Eyrolles, L., Soucé, M., Dubois, P., Chourpa, I., 2007. Comparative study of doxorubicin-loaded poly(lactide-co-glycolide) nanoparticles prepared by single and double emulsion methods. Eur. J. Pharm. Biopharm. 66, 488–492.

Trouet, A., Jolles, G., 1984. Targeting of daunorubicin by association with DNA or proteins: a review. Semin. Oncol. 11, 64–72.

Vauthier, C., Cabane, B., Labarre, D., 2008. How to concentrate nanoparticles and avoid aggregation? Eur. J. Pharm. Biopharm. 69, 466–475.

Wang, S., Deng, Y., Xu, H., Wu, H., Qiu, Y., Qiu, Y., Chen, D., 2006. Synthesis of a novel galactosylated lipid and its application to the hepatocyte-selective targeting of liposomal doxorubicin. Eur. J. Pharm. Biopharm. 62, 32–38.

Wong, H.L., Bendayan, R., Rauth, A.M., Wu, X.Y., 2004. Development of solid lipid nanoparticles containing ionically complexed chemotherapeutic drugs and chemosensitizers. J. Pharm. Sci. 93, 1993–2008.

Wong, H.L., Bndayan, R., Rauth, A.M., Li, Y., Wu, X.Y., 2007. Chemotherapy with anticancer drugs encapsulated in solid lipid nanoparticles. Adv. Drug Deliv. Rev. 59, 491–504.

Wong, H.L., Rauth, A.M., Bendayan, R., Manias, J.L., Ramaswamy, M., Liu, Z., Erhan, S.Z., Wu, X.Y., 2006. Polymer lipid hybrid nanoparticle system increases cytotoxicity of doxorubicin against multidrug-resistant human breast cancer cells. Pharm. Res. 23, 1574–1585.

Wu, J., Nantz, M.H., Zern, M.A., 2002. Targeting hepatocytes for drug and gene delivery: emerging novel approaches and applications. Front. Biosci. 7, 717–725.

Xu, Z., Chen, L., Gu, W., Gao, Y., Lin, L., Zhang, Z., Xi, Y., Li, Y., Li, 2009. The performance of docetaxel-loaded solid lipid nanoparticles targeted to hepatocellular carcinoma. Biomaterials 30, 226–232.

Zanta, M.A., Boussif, O., Adib, A., Behr, J.P., 1997. In vitro gene delivery to hepatocytes with galactosylated polytheylenimine. Bioconjug. Chem. 8, 839–844.